School of Traditional Chinese Medicine[1], Shenyang Pharmaceutical University, Shenyang; Department of Toxicology[2], School of Public Health, Tianjin Medical University, Tianjin; Translational Medicine Center[3], the First Affiliated Hospital of Liaoning Medical University, Jing Zhou, China

Structure-inhibition relationship of podophyllotoxin (PT) analogues towards UDP-glucuronosyltransferase (UGT) isoforms

Jia-Qi Qi[1,3], Yun-Feng Cao[3], Xiao-Yu Sun[3], Mo Hong[3], Zhong-Ze Fang[2], Da-Li Meng[1], Dong-Xue Sun[1]

Received September 26, 2014, accepted October 24, 2014

Zhong-Ze Fang, Department of Toxicology, School of Public Health, Tianjin Medical University, 22 Qixiangtai Road, Heping District, Tianjin 300070, China
fangzhongze@tijmu.edu.cn
Dong-Xue Sun, School of Traditional Chinese Medicine, Shenyang Pharmaceutical University, Shenyang, 110016, China
sundongxue1973@126.com
Da-Li Meng, School of Traditional Chinese Medicine, Shenyang Pharmaceutical University, Shenyang, 110016, China
wonder7141@163.com

Pharmazie 70: 239–243 (2015) *doi: 10.1691/ph.2015.4807*

UDP-glucuronosyltransferases (UGTs) are involved in the clearance of many important drugs and endogenous substances, and inhibition of UGTs' activity by herbal components might induce severe herb-drug interactions or metabolic disturbances of endogenous substances. The present study aims to determine the inhibition of UGTs' activity by podophyllotoxin derivatives, trying to indicate the potential herb-drug interaction or metabolic influence towards endogenous substances' metabolism. Recombinant UGT isoforms (except UGT1A4)-catalyzed 4-methylumbelliferone (4-MU) glucuronidation reaction and UGT1A4-catalyzed trifluoperazine (TFP) glucuronidation were employed to firstly screen the podophyllotoxin derivatives' inhibition potential. Structure-dependent inhibition behavior of podophyllotoxin derivatives towards UGT isoforms was detected. Inhibition kinetic type and parameter (K_i) were determined for the inhibition of podophyllotoxin towards UGT1A1, and competitive inhibition of podophyllotoxin towards UGT1A1 was observed with the inhibition kinetic parameter (Ki) to be 4.0 μM. Furthermore, podophyllotoxin was demonstrated to exert medium and weak inhibition potential towards human liver microsomes (HLMs)-catalyzed SN-38 glucuronidation and estradiol-3-glucuronidation. In conclusion, podophyllotoxin inhibited UGT1A1 activity, indicating potential herb-drug interactions between podophyllotoxin-containing herbs and drugs mainly undergoing UGT1A1-mediated metabolism.

1. Introduction

Podophyllotoxin and its derivatives are important lignans found in multiple plants such as Berberidaceae, Polygalaceae, Apiaceae, Linaceae, Labiaceae and Fabaceae (Imbert 1998). Since ancient times podophyllotoxin derivatives have been used as antidotes against poisons or as cathartic, purgative, antihelminthic, vesicant, and suicidal agents (Ayres and Loike 1990). They are used as an antivirals in the treatment of Condyloma acuminata, and other venereal and perianal warts (Beutner 1995). Podophyllotoxin derivatives are drawing more and more attention from researchers due to their excellent antitumor activities (Chen 2004), and two semisynthetic analogues, etoposide and teniposide, have been successfully developed for clinical use to treat cancer (Hande 1998; Johnson et al. 1991). Complex therapeutic regimens are routine in the treatment of cancers. Therefore, drug-drug interactions might also occur between podophyllotoxin derivatives and other drugs.

UDP-glucuronosyltransferases (UGTs)-catalyzed glucuronidation reaction has been demonstrated to be one of the most important metabolism processes to eliminate clinical drugs and their corresponding metabolites (Evans and Relling 1999). Additionally, the glucuronidation process is also involved in the elimination of endogenous substances, such as bilirubin, steroid hormones, thyroid hormones, bile acids and fat-soluble vitamins (Ritter 2000). Xenobiotics-induced inhibition of UGTs' activity might induce severe drug-drug interaction and even metabolic disorders of endogenous substances. For example, indinavir, a clinical drug used to fight HIV, can induce the elevation of unconjugated bilirubin in serum through inhibiting UGT1A1-catalyzed glucuronidation of bilirubin (Zucker et al. 2001). Inhibition of UGT1A1 activity by sorafenib can also induce elevation of serum bilirubin (Meza-Junco et al. 2009). Many xenobiotics have been demonstrated to exhibit medium or strong inhibition towards various UGT isoforms, such as carvacrol (Dong et al. 2012), medroxyprogesterone acetate (Huang et al. 2010), chlormadinone acetate (Huang et al. 2011), and magnolol (Zhu et al. 2012).

Podophyllotoxin derivatives are also inhibiting the important phase I drug-metabolizing enzymes cytochrome P450 3A4 and 2C9 (Song et al. 2011). Lee et al. demonstrated that deoxypodophyllotixon (DPT) was metabolized by CYP3A4 and

Table 1: Initial screening of podophyllotoxin derivatives (100 μM) towards various UGT isoforms

	PT	PT-G	4'-DEPT	4'-DEPT-G	PPT	PPT-2G	DPT
UGT1A1	19.1 ± 1.1	88.4 ± 1.8	32.3 ± 16.6	77.7 ± 0.6	66.6 ± 6.3	95.6 ± 1.4	27.4 ± 0.03
UGT1A3	99.0 ± 9.7	89.7 ± 0.8	45.8 ± 8.1	91.0 ± 4.9	103.2 ± 4.6	92.4 ± 0.1	81.7 ± 29.9
UGT1A4	53.5 ± 2.6	88.6 ± 2.0	66.3 ± 0.8	80.0 ± 1.4	71.1 ± 45.3	92.8 ± 2.0	81.4 ± 17.5
UGT1A6	74.6 ± 1.7	95.8 ± 6.2	88.2 ± 2.7	85.5 ± 3.4	84.8 ± 3.1	86.6 ± 5.6	82.8 ± 33.1
UGT1A7	62.3 ± 0.9	107.5 ± 3.3	57.2 ± 3.1	90.0 ± 0.6	71.1 ± 6.6	98.8 ± 1.1	66.9 ± 13.8
UGT1A8	74.1 ± 4.9	110.6 ± 2.4	68.2 ± 0.8	101.8 ± 0.5	76.0 ± 4.2	92.7 ± 2.6	149.5 ± 4.37
UGT1A9	95.5 ± 1.8	98.7 ± 0.2	86.9 ± 4.3	98.6 ± 4.7	100.7 ± 2.9	64.9 ± 22.5	83.9 ± 26.4
UGT1A10	60.2 ± 5.6	82.8 ± 1.6	99.5 ± 7.8	58.5 ± 0.5	73.6 ± 0.0	84.3 ± 0.4	60.7 ± 7.91
UGT2B4	111.0 ± 2.5	70.4 ± 7.4	105.5 ± 7.7	77.6 ± 5.8	81.6 ± 9.8	82.2 ± 20.5	54.2 ± 19.31
UGT2B7	52.7 ± 4.1	101.1 ± 2.3	45.7 ± 0.7	80.8 ± 7.9	83.2 ± 0.9	102.6 ± 0.5	107.9 ± 12.3

The values shown in this Table are the residual activity, which is calculated using the following equation: % residual activity = (the activity at 100 μM podophyllotoxin derivatives / the control activity at 0 μM podophyllotoxin derivatives)* 100%.

CYP2C19 in rats and HLMs and exhibited strongly competitive inhibition towards CYP3A4 and CYP2C9 (Lee et al. 2008, 2010). The recent study paid attention to the inhibitory potential of podophyllin derivatives towards UGT isoforms, aiming to indicate UGT related drug-drug interactions.

2. Investigations and results

2.1. Structure-dependent inhibition of podophyllotoxin derivatives towards various UGT isoforms

Podophyllotoxin derivatives (100 μM) were used to perform the initial inhibition screening towards various UGT isoforms, and the preliminary results are given in Table 1. The various podophyllotoxin derivatives (Fig. 1) showed different inhibition potential towards UGT isoforms. For example, the inhibition capabilities of podophyllotoxin (PT), 4'-demethhyl-podophyllotoxin (4'-DEPT) and picropodophyllotoxin (PPT) towards UGT1A1, 1A4, 1A7, 1A8 and 2B7 were stronger than those of podophyllotoxin-4-*O*-β-D-glucopyranoside (PT-G), 4'-demethhyl-podophyllotoxin-4-*O*-β-D-glucopyranoside (4'-DEPT-G) and picropodophyllotoxin-4-*O*-β-D-glucopyranosyl-(1→6)-β-D-glucopyranoside (PPT-2G), indicating that the deglycosylation process of PT-G, 4'-DEPT-G and PPT-2G can obviously increase the inhibition potential of these podophyllotoxin derivatives towards these UGT isoforms. In addition, 100 μM of PT, 4'-DEPT, PPT and DPT inhibited the activity of UGT1A1 by 80.9%, 67.7%, 33.4% and 72.6%, respectively. Through the comparison of their structures, the following conclusion can be drawn: 1) deoxygenation biotransformation of PT into DPT decreased the inhibition potential towards UGT1A1; 2) 4'-demethylation process of PT significantly decreased the

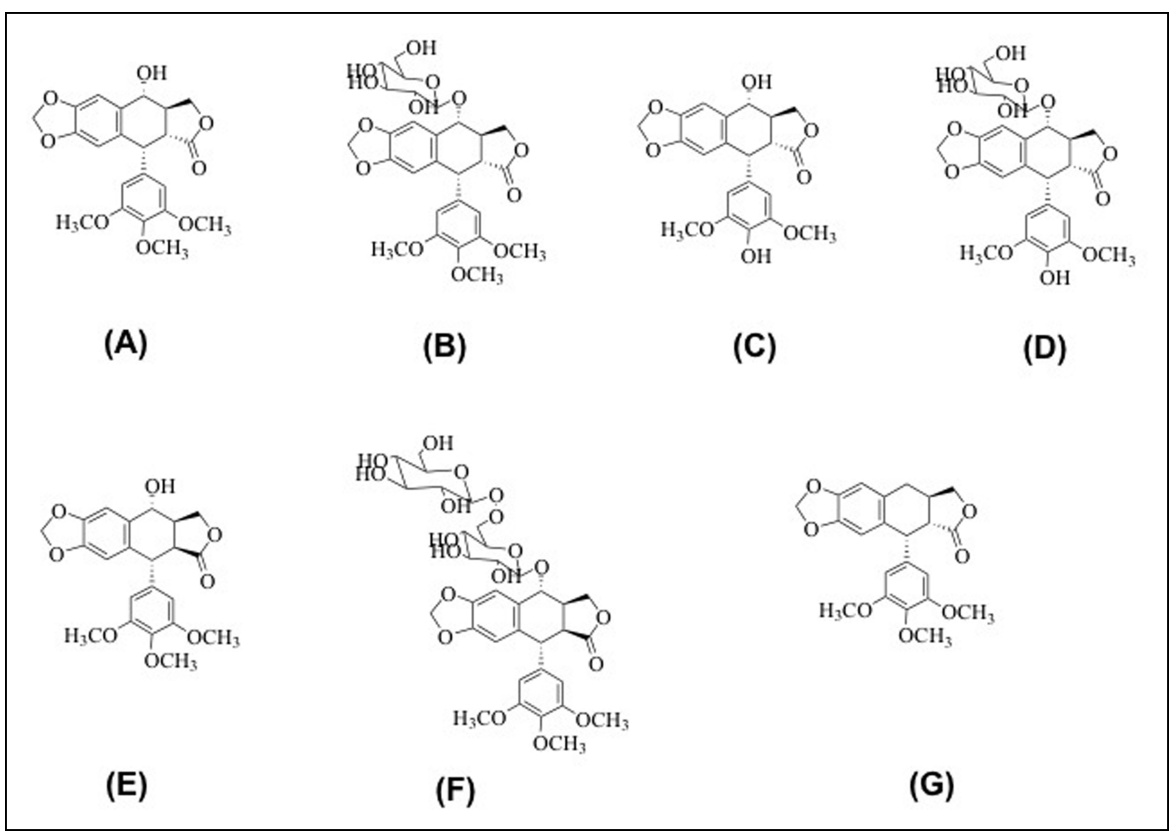

Fig. 1: Structures of podophyllotoxin derivatives. A: podophyllotoxin (PT), B: podophyllotoxin-4-O-β-D-glucopyranoside (PT-G), C: 4'-demethhyl-podophyllotoxin (4'-DEPT), D: 4'-demethhyl-podophyllotoxin-4-O-β-D-glucopyranoside (4'-DEPT-G), E: picropodophyllotoxin (PPT), F: picropodophyllotoxin-4-O-β-D-glucopyranosyl-(1→6)-β-D-glucopyranoside (PPT-2G), and G: deoxypodophyllotixon (DPT).

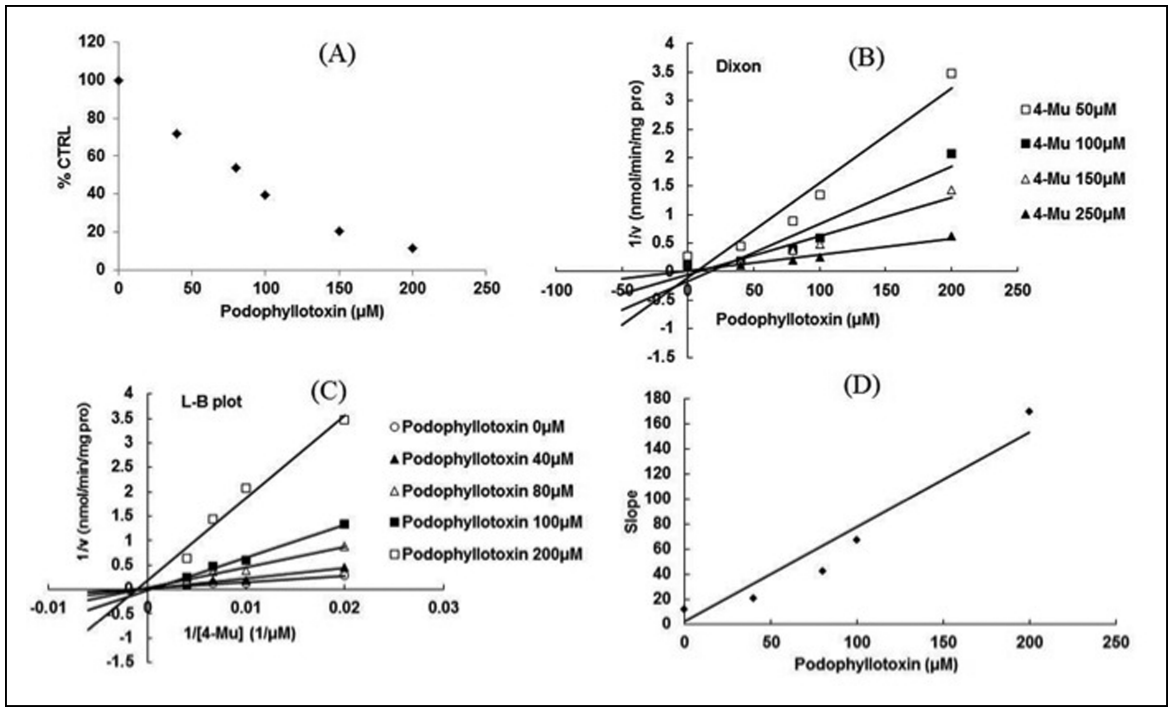

Fig. 2: Podophyllotoxin competitively inhibits recombinant UGT1A1-catalyzed 4-methylumbelliferone (4-MU) glucuronidation. (A) Dose-dependent inhibition of podophyllotoxin towards UGT1A1-catalyzed 4-methylumbelliferone (4-MU) glucuronidation; (B) Dixon plot of podophyllotoxin's inhibition towards UGT1A1-catalyzed 4-methylumbelliferone (4-MU) glucuronidation; (C) Lineweaver-Burk plot of podophyllotoxin's inhibition towards UGT1A1-catalyzed 4-methylumbelliferone (4-MU) glucuronidation. (D) Second plot of podophyllotoxin's inhibition towards UGT1A1-catalyzed 4-methylumbelliferone (4-MU) glucuronidation.

inhibition capability towards UGT1A1; 3) PPT, epimer of PT, exhibited much weaker inhibition towards UGT1A1 than PT, indicating the stereoselective inhibition towards of UGT1A1.

2.2. Podophyllotoixn exhibited competitive inhibition towards UGT1A1

The inhibition kinetic evaluation was performed for the inhibition of UGT1A1 by podophyllotoxin which inhibited UGT1A1 by more than 80% (Fig. 2) in a dose-dependend manner. Both Dixon plot and Lineweaver-Burk plot were employed to evaluate the inhibition type, and the second plot using the slopes obtained from Lineweaver–Burk plot *versus* the concentrations of podophyllotoxin was used to calculate the inhibition kinetic parameter (K_i). Based on the standard, if the intersection point was located on the vertical axis and the second quadrant in Lineweaver-Burk plot and Dixon plot, respectively, the inhibition type belongs to competitive inhibition. If the intersection point was located on the horizontal axis in both Dixon plot and Lineweaver-Burk plot, the inhibition type belongs to non-competitive inhibition. The results (Fig. 2 B&C) show that podophyllotoxin competitively inhibited UGT1A1-catalyzed 4-MU glucuronidation reaction. The inhibition kinetic parameter (K_i) was calculated to be 4.0 μM.

2.3. Substrate- and enzyme source-dependent inhibition behavior of podophyllotoxin

Substrate- and enzyme source-dependent inhibition behavior of podophyllotoxin towards UGT1A1 activity was investigated using human liver microsomes (HLMs)-catalyzed SN-38 glucuronidation and estradiol-3-glucuronidation, and the results were shown in Table 2. 1, 10, and 100 μM of PT inhibited HLM-catalyzed SN-38 glucuronidation by -9.7%, -3.8%, and 35.9%, respectively. 1, 10, and 100 μM of PT inhibited HLM-catalyzed estradiol-3-glucuronidation by 4.9%, 10.9%, and 15.9%, respectively.

Table 2: Inhibition determination of podophyllotoxin towards human liver microsomes (HLMs)-catalyzed SN-38 glucuronidation and estradiol-3-glucuronidation reaction

	SN-38	Estradiol
1 μM	109.7 ± 0.4	95.1 ± 2.3
10 μM	103.8 ± 2.9	89.1 ± 4.7
100 μM	64.1 ± 3.8	84.1 ± 8.4

1, 10, 100 μM of PT were used, and the residual activity was shown in the Table.

3. Discussion

Drug-drug interactions might result in severe clinical side effects and early termination of development, refusal of approval, severe prescribing restrictions, and withdrawal of drugs from the market. UGT1A1 is one of the most important UGT isoforms mainly distributed in human liver and intestine, and the decreased biotransformation rate might result in the adverse effects. UGT1A1 is involved in the metabolism of many important clinical drugs, and many of them have a narrow therapeutic window, such as irinotecan and etoposide (Innocenti et al. 2004; Wen et al., 2007). Additionally, the huge contribution of UGT1A1 towards the metabolism of endogenous substances makes that the inhibition of UGT1A1 activity might result in the metabolic disorders of endogenous substances (Zhang et al. 2005).

Therefore, the strong competitive inhibition of PT towards UGT1A1 activity might result in severe adverse effects, including drug-drug interactions and potential metabolic disorders. Enzyme source and substrate-dependent inhibition behavior towards UGTs have been frequently reported. For example, when 4-MU was selected as probe substrate and recombinant UGT1A9 were used, competitive inhibition was observed for the inhibition of carvacrol towards UGT1A9. However, when propofol was selected as the probe substrate, the inhi-

bition type was noncompetitive (Dong et al. 2012). In the present study, substrate and enzyme sources-dependent inhibition behavior of PT towards UGT1A1 was also observed. The inhibition of PT towards UGT1A1 became weaker when employing HLMs-catalyzed estradiol-3-glucuronidation as the probe reaction. Therefore, when extrapolating the drug-drug interaction between PT and irinotecan or the interference of PT towards endogenous substances' metabolism, this enzyme source and substrate-dependent inhibition behavior should be paid much attention.

Chemists have paid more and more interests on the structural modification to create lead compounds overcoming poor pharmacokinetic properties, including the inhibition potential towards drug-metabolizing enzymes (DMEs). Therefore, evaluating the inhibition potential of compounds with similar structures is the first key step to obtain a structure-inhibition activity relationship. Therefore, various podophyllotoxin derivatives were used in the present study to elucidate the structure-UGT inhibition relationship. The deglycosylation process of podophyllotoxin derivatives can significantly increase the inhibitory potential, which is consistent with previous reports (Guo et al. 2013). Therefore, oral administration of podophyllotoxin derivatives might exhibit stronger inhibition towards most of UGT isoforms than intravenous injection due to the deglycosylation role of the intestinal microflora. Additionally, the deoxygenation biotransformation of PT into DPT decreased the inhibition potential towards UGT1A1; 4'-demethylation process of PT significantly decreased the inhibition capability towards UGT1A1; PPT, an epimer of PT, exhibited much weaker inhibition towards UGT1A1 than PT, indicating stereoselective inhibition of UGT1A1. These structural information will help researchers to rationally design the podophyllotoxin derivatives avoiding the inhibition towards UGT isoforms.

In conclusion, structure-UGT inhibition relationship of podophyllotoxin derivatives was given in present study. A strong competitive inhibition of podophyllotoxin towards UGT1A1 was observed, and this inhibition effect depends on enzyme source and substrate.

4. Experimental

4.1. Chemicals and reagents

Podophyllotoxin derivatives were purchased from Sichuan Weikeqi Biotechnology Co. Ltd (Sichuan, China). 4-Methylumbelliferone (4-MU), Tris-HCl, 7-hydroxycoumarin and 5'-diphosphoglucuronic acid (UDPGA) (trisodium salt) were purchased from Sigma-Aldrich (Sr. Louis, MO). Recombinant human UGT supersomes (UGT1A1, UGT1A3, UGT1A6, UGT1A7, UGT1A8, UGT1A9, UGT1A10, UGT2B4, and UGT2B7) expressed in baculovirus-infected insect cells were obtained from BD Gentest Corp. (Woburn MA, USA). All other reagents were of HPLC grade or of the highest grade commercially available.

4.2. Inhibition of 4-MU glucuronidation assay

The probe substrate for all tested UGT isoforms except UGT1A4 was 4-MU which is a nonselective substrate of UGTs. The incubation and analysis conditions were performed as previously decribed (Huang et al. 2010). The mixture (200 μl total volume) contained recombinant UGTs (final concentration: 0.125, 0.05, 0.025, 0.05, 0.025, 0.05, 0.05, 0.25, and 0.05 mg/ml for UGT1A1, UGT1A3, UGT1A6, UGT1A7, UGT1A8, UGT1A9, UGT1A10, UGT2B4, and UGT2B7, respectively), 5 mM UDPGA, 5 mM $MgCl_2$, Tris-HCl buffer (PH 7.4), and 4-MU in the absence or presence of different concentrations of podophyllotoxin derivatives. The concentrations of 4-MU are: 110 μM for UGT1A1 and UGT1A6, 1200 μM for UGT1A3, 30 μM for UGT1A7, UGT1A9, and UGT1A10, 750 μM for UGT1A8, 1000 μM for UGT2B4, and 350 μM for UGT2B7. Podophyllotoxin derivatives were dissolved in methanol and the final concentration of methanol was 0.5% (v/v). After 3 min pre-incubation at 37 °C, UDPGA was added to the mixture to initiate the reaction. Incubation time was 120 min for UGT1A1, UGT1A3, UGT1A10, UGT2B4, and UGT2B7, 30 min for UGT1A6, UGT1A7, UGT1A8, and UGT1A9, respectively. The reactions were quenched by adding 100 μl acetonitrile with 7-hydroxycoummarin (100 μM) as internal standard. The mixture was centrifuged at 20,000 × g for 20 min and an aliquot of supernatant was transferred to an auto-injector vial for UFLC analysis, the Shimadzu (Kyoto, Japan) prominence ultra-fast liquid chromatography (UFLC) system contained a CBM-20A communications bus module, an SIL-20ACHT auto sampler, two LC-20AD pumps, a DGU-20A3 vacuum degasser and a CTO-20AC column oven. Chromatographic separation was carried out using a Shim-pack XR-ODS column (75 mm × 2.0 mm, 2.2 μm, Shimadzu) A SPD-20AVP UV detector (320 nm), and a flow rate of 0.4 ml/min. The mobile phase consisted of acetonitrile (A) and H_2O containing 0.2% (v/v) formic acid (B). The following gradient condition was used: 0-4 min, 95-50% B; 4-7 min, 5% B; and 7-10 min, 95% B. The calculation curve was generated by peak area ratio (4-MUG/internal standard) over the concentration range of 4-MUG 0.1-100 mM. The curve was linear over this concentration range ($r^2 > 0.99$). The limits of detection and quantification were determined at signal-to-noise ratios of 3 and 10, respectively. The accuracy and precision of the back-calculated values for each concentration were less than 5%.

4.3. Evaluation of the inhibition of podophyllotoxin derivatives towards UGT1A4-catalyzed glucuronidation of trifluoperazine (TFP)

Since UGT1A4 showed no catalytic activity towards 4-MU glucuronidation, UGT1A4-catalyzed glucuronidation of trifluopazine was selected as probe reaction for UGT1A4. Recombinant UGT1A4 (0.1 mg/ml) was incubated with 50 μM of trifluoperazine, and incubation time was 30 min. Chromatographic separation was carried out using a Shim-pack XR-ODS column (75 mm × 2.0 mm, 2.2 μm, Shimadzu) at a flow rate of 0.4 mL/min and UV detector at 256 nm. The mobile phase consisted of acetonitrile (A) and H_2O containing 0.2% (v/v) formic acid (B). The following gradient condition was used: 0-6 min, 80-30% B; 6-8 min, 10% B; and 8-12 min, 80% B.

4.4. Inhibition of podophyllotoxin towards human liver microsomes (HLMs)-catalyzed SN-38 glucuronidation and estradiol-3-glucuronidation reaction

For the inhibition of podophyllotoxin derivatives towards HLMs-catalyzed SN-38 glucuronidation, HLMs were incubated with 1.5 μM of SN-38, and incubation time was 60 min. After centrifugation at 20,000 × g for 20 min, aliquots of the supernatants were analyzed on UFLC system (Shimadzu, Kyoto, Japan) coupled with ABSCIEX 4000-QTRAP MS instrument. Phenomenex ODS column (4.6 mm × 50 mm, 3 μm) was used with a flow rate 0.4 mL/min. The mobile phase consisted of 5 mM NH4AC (A) and MeOH (B). The following gradient condition was used: 0–2 min, 75-80% B; 2–4 min, 80-95% B; 4–4:30 min, 95-75% B; 4:30-8:00 min, 75%. The MS conditions were as follows: CRU Gas, 20.0 psi; IonSpray Voltage (IS), – 4500 V; TEM, 550 °C; GS1, 55 psi; GS2, 55 psi. Negative mode was used, and the ions 390.8 and 566.8($[M–H]^-$) were used to monitor SN-38 and its glucuronide.

The inhibition of podophyllotoxin derivatives towards HLM-catalyzed estradiol-3-glucuronidation was also determined. HLM was incubated with 10 μM of estradiol, and incubation time was 60 min. After centrifugation at 20,000 × g for 20 min, aliquots of the supernatants were analyzed on UFLC system (Shimadzu, Kyoto, Japan) coupled with ABSCIEX 4000-QTRAP MS instrument. Phenomenex ODS column (4.6 mm × 50 mm, 3 μm) was used with a flow rate of 0.4 mL/min. The mobile phase consisted of 5 mM NH4AC (A) and MeOH (B). The following gradient condition was used: 0–2 min, 50-70% B; 2–3 min, 70-90% B; 3–5 min, 90% B; 5-5:30 min, 90-50%; 5:30-8:30 min, 50%. The MS conditions were as follows: CRU Gas, 20.0 psi; IonSpray Voltage (IS), – 4500 V; TEM, 500 °C; GS1, 50 psi; GS2, 50 psi. Negative mode was used, and the ions 271 and 477($[M–H]^-$) were used to monitor estradiol and its glucuronide.

4.5. Inhibition kinetic evaluation

To determine the inhibition kinetic behavior (including inhibition type and parameters), the reaction velocity was determined at various concentrations of podophyllotoxin and probe substrates. Dixon and Lineweaver–Burk plots were employed to determine theinhibition kinetic type, and the second plot with the slopes from Lineweaver–Burk plot towards the concentrations of podophyllotoxin was utilized to determine the inhibition kinetic parameters (K_i).

Acknowledgements: This research was supported by the National Natural Science Foundation of China (No. 81202586, 81202588).

Conflict of Interest: The authors have declared that there is no conflict of interest.

References

Ayres DC, Loike JD (1990) Lignans: chemical, biological and clinical properties, Cambridge University Press.

Beutner K (1995) Podophyllotoxin in the treatment of genital warts. Cur Prob Dermatol 24: 227–232.

Chen Y (2004) A fatal fibrillation atrial and coagulopathy by *Dysosma versipellis* Rhizome poisoning. Chin J Prim Med Pharm 11: 1330.

Dong RH, Fang ZZ, Zhu LL, Liang SC, Ge GB, Yang L, Liu ZY (2012) Investigation of UDP-glucuronosyltransferases (UGTs) inhibitory properties of carvacrol. Phytother Res 26: 86–90.

Evans WE, Relling MV (1999) Pharmacogenomics: translating functional genomics into rational therapeutics. Science 286: 487–491.

Galijatovic A, Otake Y, Walle UK Walle T (2001) Induction of UDP-glucuronosyltransferase UGT1A1 by the flavonoid chrysin in Caco-2 cells—potential role in carcinogen bioinactivation. Pharm Res 18: 374–379.

Guo B, Fan XR, Fang ZZ, Cao YF, Hu CM, Yang J, Zhang YY, He RR, Zhu X, Yu ZW, Sun XY, Hong M, Yang L (2013) Deglycosylation of liquiritin strongly enhances its inhibitory potential towards UDP-glucuronosyltransferase (UGT) isoforms. Phytother Res 27:1232–1236.

Hande K (1998) Etoposide: four decades of development of a topoisomerase II inhibitor. Eur J Cancer 34: 1514–1521.

Huang T, Fang Z, Yang L (2010) Strong inhibitory effect of medroxyprogesterone acetate (MPA) on UDP-glucuronosyltransferase (UGT) 2B7 might induce drug–drug interactions. Pharmazie 65: 919–921.

Huang T, Fang ZZ, Zhang YY, Zhu LL, Feng LL, Zheng W, Cao YF, Sun DX, Yang L (2011) Inhibitory potential of chlormadinone acetate (CMA) on five important UDP-glucuronosyltransferases in human liver. Pharmazie 66: 212–215.

Imbert T (1998) Discovery of podophyllotoxins. Biochimie 80: 207–222.

Innocenti F, Undevia SD, Iyer L, Chen PX, Das S, Kocherginsky M, Karrison T, Janisch L, Ramírez J, Rudin CM (2004) Genetic variants in the UDP-glucuronosyltransferase 1A1 gene predict the risk of severe neutropenia of irinotecan. J Clin Onco 22: 1382–1388.

Johnson DH, Hainsworth JD, Hande KR, Anthony Greco F (1991) Current status of etoposide in the management of small cell lung cancer. Cancer 67: 231–244.

Lee SK, Jun IH, Yoo HH, Kim JH, Seo YM, Kang MJ, Lee SH, Jeong TC, Kim DH (2008) Characterization of in vitro metabolites of deoxypodophyllotoxin in human and rat liver microsomes using liquid chromatography/tandem mass spectrometry. Rapid Commun Mass Spectrom 22: 52–58.

Lee SK, Kim Y, Jin C, Lee SH, Kang MJ, Jeong TC, Jeong SY, Kim D-H, Yoo HH (2010) Inhibitory Effects of Deoxypodophyllotoxin from < EM EMTYPE = . Planta Medica 76: 701–704.

Meza-Junco J, Chu QSC, Christensen O, Rajagopalan P, Das S, Stefanyschyn R, Sawyer MB (2009) UGT1A1 polymorphism and hyperbilirubinemia in a patient who received sorafenib. Cancer Chemoth Pharm 65: 1–4.

Ritter JK (2000) Roles of glucuronidation and UDP-glucuronosyltransferases in xenobiotic bioactivation reactions. Chem-Biological Interact 129: 171–193.

Song J-H, Sun D-X, Chen B, Ji D-H, Pu J, Xu J, Tian F-D and Guo L (2011) Inhibition of CYP3A4 and CYP2C9 by podophyllotoxin: Implication for clinical drug-drug interactions. J Biosci 36: 879–885.

Watanabe Y, Nakajima M, Ohashi N, Kume T. Yokoi T (2003) Glucuronidation of etoposide in human liver microsomes is specifically catalyzed by UDP-glucuronosyltransferase 1A1. Drug Metab Dispos 31: 589–595.

Wen Z, Tallman MN, Ali SY, Smith PC (2007) UDP-glucuronosyltransferase 1A1 is the principal enzyme responsible for etoposide glucuronidation in human liver and intestinal microsomes: structural characterization of phenolic and alcoholic glucuronides of etoposide and estimation of enzyme kinetics. Drug Metab Dispos 35: 371–380.

Zhang D, Chando TJ, Everett DW, Patten CJ, Dehal SS and Humphreys WG (2005) In vitro inhibition of UDP glucuronosyltransferases by atazanavir and other HIV protease inhibitors and the relationship of this property to in vivo bilirubin glucuronidation. Drug Metab Dispos 33: 1729–1739.

Zhu L, Ge G, Liu Y, He G, Liang S, Fang Z, Dong P, Cao Y and Yang L (2012) Potent and selective inhibition of magnolol on catalytic activities of UGT1A7 and 1A9. Xenobiotica 42: 1001–1008.

Zucker SD, Qin X, Rouster SD, Yu F, Green RM, Keshavan P, Feinberg J, Sherman KE (2001) Mechanism of indinavir-induced hyperbilirubinemia. Proc Natl Acad Sci 98: 12671–12676.